Two Cloud-Point Phenomena in Tetrabutylammonium Perfluorooctanoate Aqueous Solutions: Anomalous Temperature-Induced Phase and Structure Transitions

Peng Yan,[†] Jin Huang,[‡] Run-Chao Lu,[†] Chen Jin,[†] Jin-Xin Xiao,*[,†] and Yong-Ming Chen*[,‡]

Institute of Physical Chemistry, Peking University, Beijing 100871, China, and State Key Laboratory of Polymer Physics and Chemistry, Institute of Chemistry, The Chinese Academy of Sciences, Beijing 100080, China

Received: October 15, 2004; In Final Form: November 29, 2004

This paper reported the phase behavior and aggregate structure of tetrabutylammonium perfluorooctanoate (TBPFO), determined by differential scanning calorimeter, electrical conductivity, static/dynamic light scattering, and rheology methods. We found that above a certain concentration the TBPFO solution showed anomalous temperature-dependent phase behavior and structure transitions. Such an ionic surfactant solution exhibits two cloud points. When the temperature was increased, the solution turned from a homogeneous-phase to a liquid−liquid two-phase system, then to another homogeneous-phase, and finally to another liquid−liquid two-phase system. In the first homogeneous-phase region, the aggregates of TBPFO were rodlike micelles and the solution was Newtonian fluid. While in the second homogeneous-phase region, the aggregates of TBPFO were large wormlike micelles, and the solution behaved as pseudoplastic fluid that also exhibited viscoelastic behavior. We thought that the first cloud point might be caused by the "bridge" effect of the tetrabutylammonium counterion between the micelles and the second one by the formation of the micellar network.

Introduction

Surfactants can spontaneously form various aggregates in aqueous solution, such as micelle, vesicle, and liquid crystal, because of their amphiphilic nature.[1] Temperature is one of the important factors that dominate the formation of surfactant aggregates. It is well-known that below the Krafft point ionic surfactants could not form micelles.[2] On the contrary, the aqueous micellar solution of nonionic surfactants exhibits lower consolute temperature, also called cloud point. Above the cloud point the micellar solution spontaneously separates into two distinct phases, one phase is surfactant-enriched and the other is surfactant-depleted.[2]

The mechanism of the lower consolute behavior in nonionic surfactant systems has not been exactly known. Previous researches thought that the phase separation might be due to the micellar growth, the micellar coacervation, or the changes in poly(oxyethylene) chain conformations with temperature.[3−5] Recent experimental and theoretical investigations showed that the formation of the connected micellar network[6−8] or the strongly orientation-dependent interactions (H bonds) between water and the surfactant molecules[9] could be responsible for the lower consolute behavior. Generally, the lower consolute behavior would not happen in ionic surfactant systems because of the significant electrostatic repulsions between the charged aggregates. Nevertheless, previous researches showed that aqueous solutions of some ionic surfactants with high salt concentration,[10−14] salt free aqueous solutions of certain ionic surfactants with large headgroups[15,16] or large counterions,[17−19] and some mixed cationic and anionic surfactant solutions[20] also exhibited the lower consolute behavior. The mechanism of the lower consolute behavior in these ionic surfactant solutions is still an open question.[13,19,21,22]

In this work, we found that the aqueous solution of tetrabutylammonium perfluorooctanoate (TBPFO), an anionic fluorinated surfactant, not only exhibited the lower consolute behavior, but also showed two cloud points when the temperature was increased. These novel two cloud-point phenomena were found in certain nonionic surfactant[23] and nonionic block polymer;[24] however, researches showed the two cloud points in those systems were attributed to the presence of impurity with higher hydrophobicity.[23,24] The more hydrophobic impurity was caused by the polydispersed preparations of the nonionic surfactant and block polymer. In this work, the more hydrophobic impurity could be avoided when ionic surfactant with small molecular weight was used. The present work was focused on the phase behavior and aggregate structure of TBPFO solution using differential scanning calorimeter, electrical conductivity, static/dynamic light scattering, and rheology methods.

Materials and Methods

Perfluorooctanoic acid and tetrabutylammonium hydroxide were obtained from Acros Organics and Beijing Chemical Co., respectively. Tetrabutylammonium perfluorooctanoate (TBPFO) was prepared by neutralizing perfluorooctanoic acid with tetrabutylammonium hydroxide. The purity of the surfactant was examined, and no minima were observed in the surface tension curves, indicating the absence of surface-active impurity.

To determine the cloud point, TBPFO solutions were approximately cooled to 4 °C, then placed in a thermal bath and slowly heated. The cloud point was regard as an abrupt clouding of the solution observed visually. The cloud point was determined three times and the relative error was less than 0.2 °C.

* To whom correspondence should be addressed. E-mail: xiaojinxin@pku.edu.cn; ymchen@iccas.ac.cn

[†] Peking University.

[‡] The Chinese Academy of Sciences.

10.1021/jp045283m CCC: $30.25
Published on Web 03/01/2005

The electrical conductivity measurements of the surfactant solutions were performed on a Jenway model 4320 conductivity meter at 25 °C.

Differential scanning calorimeter (DSC) measurements were carried out at 0.2 °C/min usinga Micro DCS III (Setaram-France) instrument. The solutions were degassed under reduced pressure before the measurements.

For light-scattering experiments, all solutions were filtered through a 0.2 μm ArcoDisk filter into the cylindrical scattering cells at about 4 °C. Static/dynamic light scattering (SLS/DLS) experiments were performed on a spectrometer of standard design by means of an ALV-5000/E/WIN Multiple Tau Digital correlator, a Spectra-Physics 2017 200-mW Ar laser (514.5-nm wavelength), a computer-controlled and stepping-motor-driven variable angel detection system, and a temperature-controlled sample cell.

Based on the static light scattering theory in the dilute macromolecule solution or colloidal suspension,[25,26] the angular dependence of excess absolute average scattered intensity, also known as the excess Rayleigh ratio $R_{ex}(\theta)$, can be expressed as

$$\frac{KC}{R_{ex}(\theta)} \cong \frac{1}{M_{w,app}}\left(1 + \frac{\langle R_g^2\rangle q^2}{3}\right) \quad (1)$$

where $K = 4\pi^2 n^2 (\partial n/\partial C)^2/(N_A \lambda_0^4)$ with N_A, n, and λ_0 being Avogadro's number, the solvent refractive index, and the wavelength of light in vacuo, respectively, and $q = (4\pi n/\lambda_0)\sin(\theta/2)$ with θ being the scattering angle. The apparent weight-average molecular weight, $M_{w,app}$, is obtained from the intercept when $KC/R_{ex}(\theta)$ is plotted versus q^2. From the $M_{w,app}$, we can determine the apparent aggregation number, $N_{agg,app}$, of the TBPFO aggregates. However, it is difficult for us to obtain the accurate values of aggregation number from the SLS experiments, because the effect of the interactions between the aggregates cannot be neglected. For the polymer systems, this difficulty can be overcome by extrapolating the experimental data to zero concentration. But, this treatment cannot be applied to the case of surfactant systems, since the molecular weight or aggregation number of the aggregates largely depends on the surfactant concentration.

The hydrodynamic properties of the TBPFO aggregates can be characterized by DLS.[27] The intensity−intensity time correlation function $G^{(2)}(q,t)$ was measured, which has the form

$$G^{(2)}(q,t) = A + B|g^{(1)}(q,t)|^2 \quad (2)$$

where A, B, and $g^{(1)}(q,t)$ are a measured baseline, an optical constant of the system, and the normalized electric field (E) time correlation function, respectively. It has been shown that $g^{(1)}(q,t)$ can be related to the line-width distribution $G(\Gamma)$ by

$$g^{(1)}(q,t) = \int_0^\infty G(\Gamma)e^{-\Gamma_t}\,d\Gamma \quad (3)$$

The Laplace inversion of eq 3, done by the CONTIN program[28] supplied with the ALV-5000 digital time correlator, was used in the determination of $G(\Gamma)$. For a diffusive relaxation, Γ is normally a function of both C and θ, which can be expressed as

$$\Gamma/q^2 = D(1 + k_d C)(1 + f\langle R_g^2\rangle_z q^2) \quad (4)$$

where k_d is the diffusion second virial coefficient and f is a dimensionless number. At $C \to 0$ and $\theta \to 0$, $\Gamma/q^2 \to D$. Therefore, $G(\Gamma)$ obtained can be transferred into a translational diffusion coefficient distribution $G(D)$. Furthermore, $G(D)$ can be converted into a hydrodynamic radii distribution $f(R_h)$ by using the well-known Stokes−Einstein equation

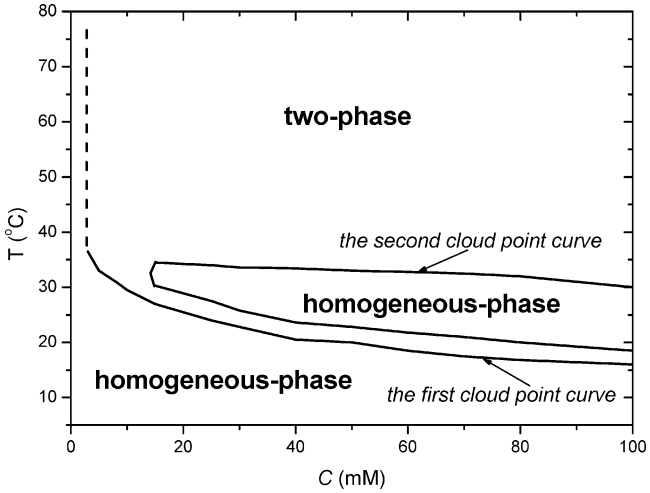

Figure 1. The lower consolute behavior in tetrabutylammonium perfluorooctanoate (TBPFO) aqueous solution.

$$R_h = \frac{k_B T}{6\pi\eta D} \quad (5)$$

where k_B, T, and η are the Boltzmann constant, the absolute temperature, and the solvent viscosity at T, respectively. The Stokes−Einstein equation is only strictly valid for spheral particles. When the particle is nonspheral, what we obtain from the Stokes−Einstein equation is the apparent hydrodynamic radius, or the equivalent radius corresponding to a sphere of the same diffusion coefficient.

The rheology experiments were measured with a Thermo-Haake RS300 rheometer. A double gap cylinder sensor system with an outside gap of 0.30 mm and an inside gap of 0.25 mm was used. Steady shear measurements were performed in the shear rate range $\dot{\gamma} = 0.1-2000\ s^{-1}$. Dynamic measurements were carried out for angular frequencies $\omega = 0.1-100$ rad·s^{-1}.

Results and Discussion

Figure 1 shows the partial phase diagram of the TBPFO−water system. It was observed that the TBPFO−water system exhibited lower consolute behavior when the concentration exceeded critical micellar concentration (cmc), 2.3 mM at 25 °C. At the concentration between cmc and 15 mM, this ionic surfactant behaved like common nonionic surfactants, the solution has one lower consolute temperature (cloud point). Dramatically, when the concentration was above a certain level, approximately 15 mM, TBPFO solution exhibited two cloud points. In the two-cloud point region, when the temperature was increased, TBPFO solution turned from a transparent homogeneous-phase to a liquid−liquid two-phase, then to another homogeneous-phase, and finally to another liquid−liquid two-phase. The temperature range of the first two-phase region was small, approximately 2−3 °C. The second cloud point also deceased with increasing surfactant concentration, but the variation of the temperature was much smaller than that of the first cloud point. With continued heating once the temperature was above the second cloud point, the solution was still a liquid−liquid two-phase. Additionally, both of the phase separations were entirely reversible when the solutions were cooled.

The phase transition can also be confirmed by the electrical conductivity measurements.[29,30] Figure 2 shows the variation

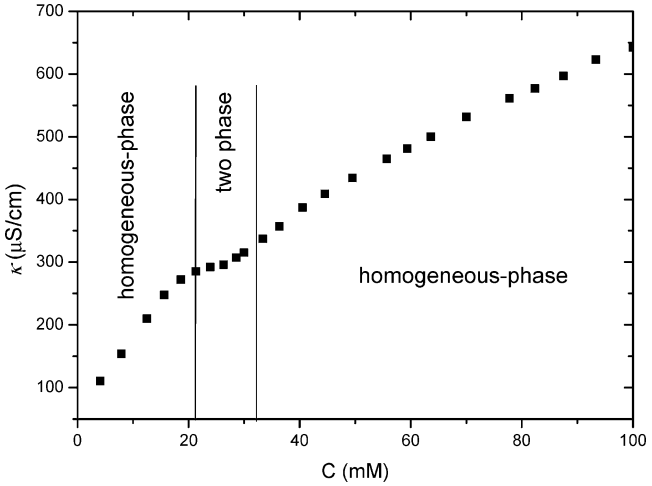

Figure 2. Variation of electrical conductivity (κ) versus TBPFO concentration at 25 °C.

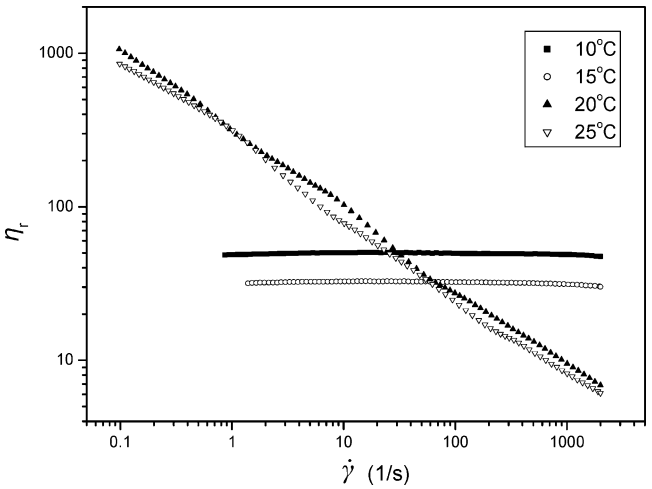

Figure 3. Relative viscosity (η_r, $\eta_r = \eta/\eta_0$, η and η_0 stand for the viscosity of the solution and solvent, respectively) of the TBPFO solution (100 mM) at different homogeneous-phase regions. At 10 and 15 °C, the TBPFO solution is in the first homogeneous region, while at 20 and 25 °C, the TBPFO solution is in the second homogeneous region.

of electrical conductivity (κ) versus the TBPFO concentration (c) at 25 °C. The phase boundary determined by electrical conductivity was generally consistent with that in Figure 1. The values of κ in the two homogeneous-phase regions are approximately linearly increased with c. Furthermore, the slopes of κ in the two homogeneous-phase regions are quite different, which suggests the aggregate structures of TBPFO are not the same in these two regions.[31]

In both of the two-phase regions, two liquidlike phases coexist, and no birefringence (by polarizers) was observed in both bottom and up phases. The bottom phase is surfactant-enriched, while the up phase is surfactant-depleted, which is quite similar to the two phases of nonionic surfactants formed above the cloud point temperatures.[2]

However, the two homogeneous-phases were quite different, which could be illustrated by the rheological and light-scattering experiments.

Figure 3 shows the relative viscosity (η_r, $\eta_r = \eta/\eta_0$, η and η_0 stand for the viscosity of the solution and solvent, respectively) of the TBPFO solution (100 mM) at different homogeneous-phase regions. In the first homogeneous-phase region (at low temperature), η_r did not change in the experimental shear rate

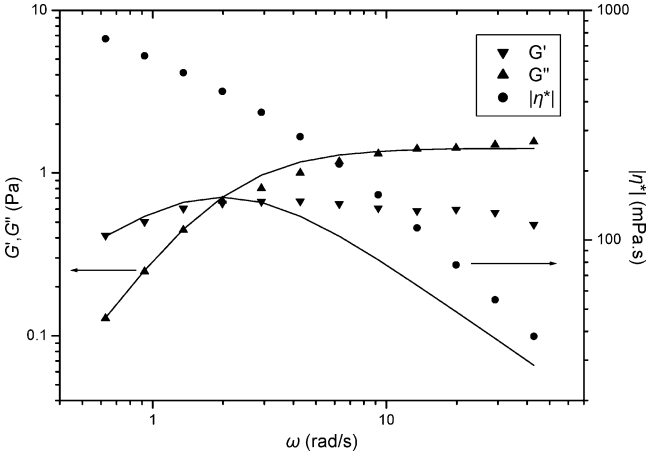

Figure 4. The storage moduli $G'(\omega)$, loss moduli $G''(\omega)$, and complex viscosity $|\eta^*|(\omega)$ of the TBPFO solution (100 mM) at 25 °C (the second homogeneous region). A simple Maxwell model fitting is shown by solid lines.

range, which indicated that the TBPFO solution was a Newtonian fluid, while in the second homogeneous-phase region (at high temperature), η_r deceased with increasing shear rate and did not exhibit any detectable yield stress value, which meant that the solution behaved as a pseudoplastic fluid. Furthermore, the TBPFO solution in the second homogeneous-phase region also exhibited viscoelastic properties. Figure 4 shows the storage moduli $G'(\omega)$, the loss moduli $G''(\omega)$, and the complex viscosity $|\eta^*|(\omega)$ of the TBPFO solution (100 mM, $T = 25$ °C). At low angular frequencies, the behavior of the TBPFO solution could be well described by the simple Maxwell model:[32]

$$G'(\omega) = G_0\frac{\omega^2\tau_0^2}{1+\omega^2\tau_0^2}, \qquad G''(\omega) = G_0\frac{\omega\tau_0}{1+\omega^2\tau_0^2} \quad (6)$$

where ω, G_0, and τ_0 are the angular frequency, plateau modulus, and relaxation time, respectively. However, at high angular frequencies $G'(\omega)$ values deviate upward from eq 6. Generally, there are three types of viscoelastic surfactant solutions,[33] which contain wormlike micelles, vesicles/classical lamellar phases, and small rodlike micelles, respectively. Obviously, aggregates of TBPFO in the second homogeneous-phase region are not the third type, because quite large aggregates were found in this region by light-scattering measurements (see below). In the second type of viscoelastic surfactant solutions, it was shown that both $G'(\omega)$ and $G''(\omega)$ were generally independent with ω and could not be described by the simple Maxwell model,[33] which were quite different from our results. Furthermore, no birefringence and vesicle (by negatively stained TEM) were found in the second homogeneous-phase region, which also indicated that aggregates of TBPFO in this region were not the second type. It is well-known that the existence of a transient network formed by the entanglement of the wormlike micelles may be responsible for the viscoelastic properties.[32−34] Therefore, we considered that, in this work, wormlike micelles might exist in the second homogeneous-phase region. Additionally, the deviation of $G'(\omega)$ at high angular frequencies indicated that the TBPFO wormlike micelles had relaxation modes much faster than the terminal modes, which might be caused by the effect of "breathing" or local Rouse motion.[35]

DLS and SLS are powerful nondestructive methods to investigate the structures of surfactant aggregates. It is shown in Figure 5 that, in the first homogeneous-phase region (TBPFO

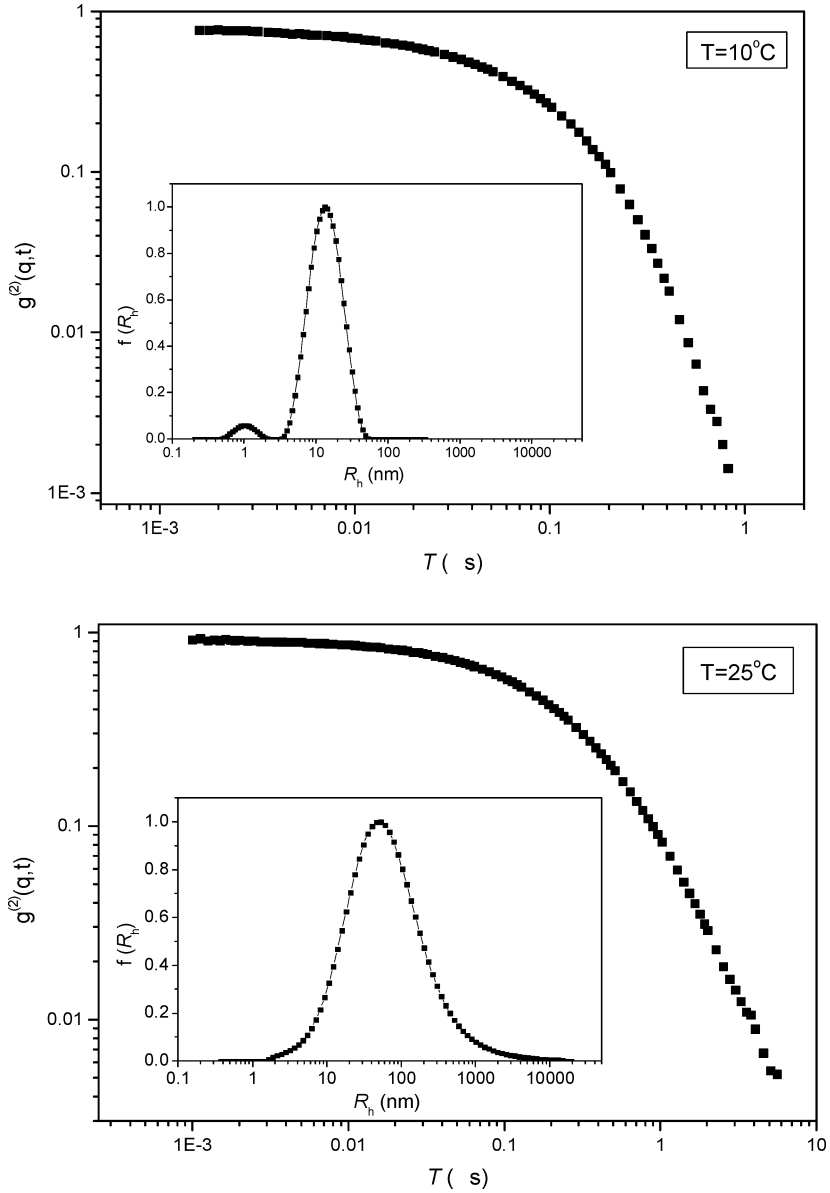

Figure 5. The intensity−intensity time correlation function ($g^{(2)}(q,t)$) of the TBPFO solution (100 mM) at different homogeneous-phase regions (scattering angle 90°). The insets are the apparent hydrodynamic radii (R_h) distribution ($f(R_h)$) of the TBPFO aggregates. At 10 °C, the TBPFO solution is in the first homogeneous region, while at 25 °C, the TBPFO solution is in the second homogeneous region.

100 mM, $T = 10$ °C), the aggregates of TBPFO are narrowly distributed, and the average apparent hydrodynamic radii (R_h) were about 10 nm (the particles with R_h about 1 nm in Figure 5 might be the tetrabutylammonium counterion (TBA^+)), while in the second homogeneous-phase region (TBPFO 100 mM, $T = 25$ °C), the aggregates of TBPFO are widely distributed, and the range of R_h was from several nanometers to several micrometers. SLS results (Table 1) indicated that the apparent aggregation number was approximately 90−100 in the first homogeneous-phase region, which meant that the aggregates of the TBPFO might be mainly rodlike micelles. Simultaneously, in the second homogeneous-phase region, the apparent aggregation number was about 2300−3400, indicating the existence of large aggregates. Combined with the rheology results we concluded that the aggregates of TBPFO in the first and second homogeneous-phase region might be rodlike and wormlike micelles, respectively.

The phase transitions always result in a thermal effect. Therefore, DSC measurements were preformed on the TBPFO solutions. Figure 6 shows that there are two endothermic peaks when the TBPFO concentration is above 15 mM, and the corresponding temperatures of the two peaks are generally in accord with the two cloud points, respectively. When the TBPFO concentration was 10 mM, only one endothermic peak was observed, which also agreed with the corresponding cloud point. So, both of the phase separations are endothermic or, in other words, entropy-driven processes. Furthermore, the area of the first endothermic peak is much smaller than that of the second

TABLE 1: The Apparent Molecular Weight ($M_{app,w}$) and Apparent Aggregation Number (N_{app}) of the TBPFO Solution (100 mM) at Different Temperatures[a]

temp (°C)	$M_{app,w}$	N_{app}
10	$6.02 \pm 0.11 \times 10^4$	92 ± 2
15	$6.25 \pm 0.19 \times 10^4$	95 ± 3
20	$1.53 \pm 0.05 \times 10^6$	$2.34 \pm 0.08 \times 10^3$
25	$2.23 \pm 0.13 \times 10^6$	$3.40 \pm 0.20 \times 10^3$

[a] At 10 and 15 °C, the TBPFO solution is in the first homogeneous region, while at 20 and 25 °C, the TBPFO solution is in the second homogeneous region.

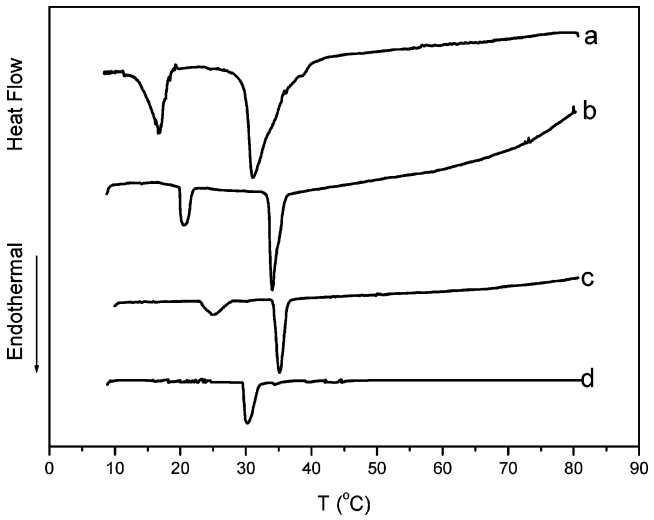

Figure 6. DSC curves of TBPFO solution with different concentrations: (a) 100, (b) 50, (c) 25, and (d) 10 mM.

peak, indicating that the thermal effects of the phase separations at the two cloud points are different. Therefore, the mechanisms of the two cloud points might not be the same.

We first consider the phase separation at the first cloud point. TBA^+ possesses four butyl chains with a symmetry structure and a positive charge on the nitrogen atom. Because of the hydrophobicity of the four butyl chains, TBA^+ might partially penetrate into the micellar interior by hydrophobic interaction. Previous researches also suggested that the penetration of TBA^+ was possible.[17,19] The penetration of the TBA^+ reduces the effective charge on the micellar surface and the electrostatic repulsions between the micelles. Since TBA^+ has the tetrahedron structure, there must be at least one butyl chain stretching outside the micellar surface, which could interact hydrophobically with butyl chains bound on the other micellar surface. Recently, Zana et al. suggested that there was a second layer of TBA^+ loosely attached outside the polar shell of the tetrabutylammonium dodecyl sulfate micelle.[36] If the second layer of TBA^+ also exists in the TBPFO micelles, the cross-linking between micelles could also take place between butyl groups of the TBA^+ ions in the second layer. In other words, TBA^+ might act like bridges linking micelles together.[17,19] As already mentioned, when the temperature was lower than the first cloud point, the TBPFO aggregate was rodlike micelles whose size was generally independent of the temperature. Therefore, the first cloud point is not caused by the micellar growth, and the cross-linking between micelles might result in the coacervation of the TBPFO micelles, which might be responsible for the phase separation of the TBPFO solution.

Then, we consider the phase separation at the second cloud point. As already mentioned, the solution in the second homogeneous phase region contains wormlike micelles. When the temperature is increased, the wormlike micelles could entangle or branch and gradually form a connected network. The formation of the connected micellar network might also contribute to the hydrophobic interaction between TBA^+.[37,38] The interaction between TBA^+ would decease their contribution to the electrical conductivity, which accords with the electrical conductivity results in this work that the slope of κ in the second homogeneous-phase region is smaller than that in the first homogeneous-phase region (small rodlike micelles without connect to each other). The configurational entropy of the network is temperature dependent.[8] At higher temperature, the system becomes unstable and separates into a dense phase in equilibrium with a dilute phase.[8] The presence of the wormlike micelle and micellar network, when the system was in the second homogeneous region, was confirmed by the DLS/SLS and rheology experiments. Previous experimental and theoretical researches have shown that phase separation in the wormlike micelle system was caused by the formation of a connected micellar network.[7,8,21]

Conclusion

Anomalous temperature-dependent phase behavior was found in TBPFO aqueous solutions. When the concentration was above a certain level, with the increase of the temperature, the TBPFO solution passed through a homogeneous-phase, a liquid−liquid two-phase, another homogeneous-phase, and another liquid−liquid two-phase, orderly, that is, such an ionic surfactant solution has two cloud points. In the first and second homogeneous-phase region, the TBPFO aggregates were quite different, in which rodlike and wormlike micelles might exist, respectively. The mechanisms of the two cloud points are not the same, and we thought that the special characteristics of TBA^+ might play a key role in the phase separations at the two cloud points.

Acknowledgment. This project was financially supported by National Natural Science Foundation of China (No 20273006).

Supporting Information Available: Determination of cmc, binding degree of counterions, surfactant concentration in the two phases, and static light scattering data of the TBPFO solution. This material is available free of charge via the Internet at http://pubs.acs.org.

References and Notes

(1) Gelbart, W. M.; Ben-Shaul, A. *J. Phys. Chem.* **1996**, *100*, 13169.
(2) Laughlin, R. G. *Handbook of Detergents Part A*: *Properties*; Broze, G., Ed.; Marcel Dekker: New York, 1999; Chapter 4.
(3) Triolo, R.; Magid, L. J.; Johnson, J. S., Jr.; Child, H. R. *J. Phys. Chem.* **1982**, *86*, 3689.
(4) Corti, M.; Minero, C.; Degiorgio, V. *J. Phys. Chem.* **1984**, *88*, 309.
(5) Lindman, B.; Carlsson, A.; Karlstrom; Malmsten, M. *Adv. Colloid Polym. Sci.* **1990**, *32*, 183.
(6) Bernheim-Groswasser, A.; Wachtel, E.; Talmon, Y. *Langmuir* **2000**, *16*, 4131.
(7) Zliman, A.; Tlusty, T.; Safran, S. A. *J. Phys.*: *Condens. Matter* **2003**, *15*, S57.
(8) Zliman, A.; Safran, S. A.; Sottmann, T.; Strey, R. *Langmuir* **2004**, *20*, 2199.
(9) Bock, H.; Gubbins, K. E. *Phys. Rev. Lett.* **2004**, *92*, 135701.
(10) Porte, G.; Appell, J. *J. Phys. Lett.* **1984**, *44*, L-689.
(11) Gomati, R.; Appell, J.; Bassereau, P.; Marignan, J.; Porte, G. *J. Phys. Chem.* **1987**, *91*, 6203.
(12) Yu, Z.-J.; Neuman, R. D. *Langmuir* **1994**, *10*, 377.
(13) Raghavan, S. R.; Edlund, H.; Kaler, E. W. *Langmuir* **2002**, *18*, 1056.
(14) Kumar, S.; Sharma, D.; Kabir-ud-Din *Langmuir* **2003**, *19*, 3539.
(15) Warr, G. G.; Zemb, T. N.; Drifford, M. *J. Phys. Chem.* **1990**, *94*, 3086.
(16) Buckingham, S. A.; Garvey, C. J.; Warr, G. G. *J. Phys. Chem.* **1993**, *97*, 10236.
(17) Yu, Z.-J.; Xu, G. *J. Phys. Chem.* **1989**, *93*, 7441.
(18) Smith, A. M.; Holmes, M. C.; Pitt, A.; Harrison, W.; Tiddy, G. J. T. *Langmuir* **1995**, *11*, 4202.
(19) Bales, B. L.; Zana, R. *Langmuir* **2004**, *20*, 1579.
(20) Xiao, J.-X.; Zhao, G.-X. *Chinese J. Chem.* **1994**, *12*, 552.
(21) Drye, T. J.; Cates, M. E. *J. Chem. Phys.* **1991**, *96*, 1367.
(22) PaniZZa, P.; Cristobal, G.; Curely, J. *J. Phys.*: *Condens. Matter* **1998**, *10*, 11659.
(23) Nakagawa, T. *Nonionic Surfactants*; Schick, M. J., Ed.; Marcel Dekker: New York, 1967; Chapter 17.

(24) Desai, P. R.; Jain, N. J.; Bahadur, P. *Colloids Surf. A* **2002**, *197*, 19.
(25) Zimm, B. H. *J. Chem. Phys.* **1948**, *16*, 1099.
(26) Debye, P. *J. Phys. Colloid Chem.* **1947**, *51*, 18.
(27) Chu, B. *Laser Light Scattering*, 2nd ed.; Academic Press: New York, 1991.
(28) Provencher, S. W. *Makromol. Chem.* **1979**, *180*, 201.
(29) Hao, J.; Hoffmann, H.; Horbaschek, K. *J. Phys. Chem. B* **2000**, *104*, 10144.
(30) Hao, J.; Yuan, Z.; Liu, W.; Hoffmann, H. *J. Phys. Chem. B* **2004**, *108*, 5105.
(31) González-Pérez, A.; Czapkiewicz, J.; Prieto, G.; Rodríguez, J. R. *Colloid Polym. Sci.* **2003**, *281*, 1191.
(32) Rehage, H.; Hoffmann, H. *Mol. Phys.* **1991**, *74*, 933.
(33) Hoffmann, H. *Structure-Performance Relationships in Surfactants*, 2nd ed.; Esumi, K., Ueno, M., Eds.; Marcel Dekker: New York, 2003; Chapter 10.
(34) Cates, M. E.; Candau, S. J. *J. Phys.*: *Condens. Matter* **1990**, *2*, 6869.
(35) Doi, M.; Edwards, S. F. *The Theory of Polymer Dynamics*; Clarendon Press: Oxford, UK, 1986.
(36) Benrraou, M.; Bales, B. L.; Zana, R. *J. Phys. Chem. B* **2003**, *107*, 13432.
(37) Watanabe, H.; Sato, T.; Osaki, K.; Matsumoto, M.; Bossev, D.; McNamee, C. E.; Nakahara, M. *Rheol. Acta* **2000**, *39*, 110.
(38) Zana, R.; Benrraou, M.; Bales, B. L. *J. Phys. Chem. B* **2004**, *108*, 18195.